

Closing the gap between wind energy targets and implementation for emerging countries



Paolo Giani^{a,*}, Felipe Tagle^b, Marc G. Genton^c, Stefano Castruccio^b, Paola Crippa^a

^a Department of Civil and Environmental Engineering and Earth Sciences, University of Notre Dame, Notre Dame, IN, USA

^b Department of Applied and Computational Mathematics and Statistics, University of Notre Dame, Notre Dame, IN, USA

^c Statistics Program, King Abdullah University of Science and Technology, Thuwal, Saudi Arabia

HIGHLIGHTS

- We provide scientific support for the deployment of wind energy infrastructure.
- A general methodology to identify optimal wind farm sites is proposed.
- A procedure to identify the most suitable wind turbine model/height is illustrated.
- A blueprint for achieving Saudi Arabia's wind energy targets is presented.
- Saudi Arabia is well positioned to be an important player in the wind energy sector.

ARTICLE INFO

Keywords:

Wind energy
WRF model
Levelized cost of energy
Wind power potential assessment
Energy policy
Saudi Arabia

ABSTRACT

Policymakers worldwide have set challenging sustainable energy targets to decarbonize their economy. Despite the ambitious pledges, several emerging countries still lack an actual progress towards the envisioned goals, often due to the scarcity of accurate data. Here, we propose a practical methodology for bridging the gap between the wind energy targets and their implementation. We illustrate our new methodology by focusing on Saudi Arabia, which endeavors to play a leading role in the renewable energy sector and pledges to install 16GW of wind capacity by 2030. We propose a blueprint for the optimal wind farms buildout, combining novel high-resolution model simulations, a unique set of observations, land-use restrictions and a thorough cost assessment. The most suitable technological option is selected among multiple turbine models for each potential site. Our findings suggest that Saudi Arabia is well positioned to become a role model for wind energy development within the Middle East, with 26% of the electricity demand that could be met by wind power. The average levelized cost of energy of the proposed buildout is 39 USD MWh⁻¹, which confirms the competitiveness of wind resources in Saudi Arabia. We identify the area close to Gulf of Aqaba as the most cost-effective region for wind harvesting, with turbines characterized by moderate specific rating (350 W m⁻²) at relatively low hub height (75 m). The modelling framework proposed in this work can be adopted by other countries aiming to start or strengthen their wind energy portfolio.

1. Introduction

The adverse impacts of burning fossil fuels on the environment and human health are well established [1] and call for profound transformations of current energy systems [2]. To reduce the dependence on non-renewable fossil fuels and comply with the long-term temperature goals of the Paris agreement, policymakers worldwide are proposing mitigating strategies and promoting renewable energy resources [3].

Among these, wind energy has seen the largest global deployment in terms of power generating capacity, with China and the United States being the major contributors [4]. Despite a lower total installed capacity, several European countries already have a large share of wind energy in their electricity generation mix. According to the latest Global Status Report of Renewables [4], at least seven European countries met 15% or more of their annual electricity demand with wind energy in 2018. For the United States, projections show that the electricity

* Corresponding author at: Department of Civil and Environmental Engineering and Earth Sciences, 267A Fitzpatrick Hall, University of Notre Dame, Notre Dame, IN 46556, USA.

E-mail address: pgiani@nd.edu (P. Giani).

produced from renewable energy sources will most likely surpass coal by 2030, with wind playing a central role [5]. On the other hand, several emerging countries have also pledged ambitious wind energy targets but an actual progress towards the envisioned goals is often missing. Some technical limitations, such as lack of standard certifications [6] and skilled personnel [7], can hinder the implementation of governments' policies. However, the major barrier to the deployment of the wind energy infrastructure is often related to the lack of accurate data and information, as for instance highlighted by previous studies in Oman [8] and Pakistan [9], along with social and political matters [10]. Whilst several studies properly quantified wind energy resources in the developed world, based on different combinations of reanalysis data [11], numerical weather prediction (NWP) model simulations [12] and ground observations [13], few detailed studies focused extensively on emerging countries [14]. Essential information spans from high-resolution mapping of wind resources and suitable technologies to the determination of economic and environmental benefits resulting from the implementation of wind farms.

Here, we introduce a new modelling framework to provide the necessary scientific support and clear, actionable cost/benefit plans for the implementation of wind targets envisioned by a country. We identify Saudi Arabia as an optimal case study given its position as an emerging country and its recent large commitment to the sustainable development goals [15]. Despite the abundance of fossil fuels in the country, in 2012 Saudi Arabia unveiled targets of 25 GW of concentrated solar power (CSP), 16 GW of solar photovoltaic (PV) and 9 GW of wind energy by 2032 [16]. More recently, as part of their 'Vision 2030' reform plan [17], Saudi Arabia upwardly revised targets to 2.7 GW of CSP, 40 GW of solar PV and 16 GW of wind [18], thereby reaffirming its commitment to transition to renewable energy sources. Although these measures would place Saudi Arabia not only at the forefront regionally in terms of capacity, but also as a leading player worldwide [19], there is still a large gap between the ambitious renewable goals and the scientific work to support them. At present, the first onshore utility-scale wind project has achieved financial close and is under construction in Dumat Al Jandal, in the North Western province of Al Jouf, and it is expected to become operative in the first quarter of 2022 [20]. Even though Dumat Al Jandal wind farm will be the largest in the Middle East, with an installed capacity of 400 MW [21], it will account for only 2.5% of the total installed capacity target set by 'Vision 2030' (16 GW).

Previous studies of wind energy potential over Saudi Arabia have mostly relied on reanalysis data, given the sparsity and low quality of observational data sources. For instance, Rehman et al. [22] analyzed wind speed data for five coastal locations and provided preliminary energy calculations for different wind turbines. Yip et al. [23] used the Modern-Era Retrospective analysis for Research and Applications (MERRA) product to examine the variability and persistence of the wind resource of the Arabian Peninsula. Chen et al. [24] considered climate model outputs to identify areas of high wind energy potential over the western part of the country and to quantify their reliability under current and future climate. Tagle et al. [25] examined the interannual variability of the wind power density using an ensemble of simulations based on using 30 simulations from the Large Ensemble Project (LENS) developed at the National Center for Atmospheric Research [26]. Tagle et al. [27] proposed a spatiotemporal stochastic generator of wind speeds to properly characterize the uncertainty of the energy estimates. Although these studies provided significant advancements in quantifying the wind energy potential over the region, actionable recommendations to policymakers are still limited due to the rather coarse resolution of the wind data and the lack of discussion of technological options.

The novelty of this work lies therefore in its effort to support the governments' initiatives by setting forth a practical strategy for implementing wind energy visions. Specifically this study seeks to overcome limitations of prior research by addressing the following

objectives:

- 1) Bridging the gap between the wind energy targets and their implementation, by providing a new general methodology for a large-scale assessment (e.g., nationwide) of wind energy resources which produces a cost-efficient blueprint for the implementation of the wind power capacity targets.
- 2) Overcoming issues of coarse resolution and/or data sparsity by combining multi-year wind speed observations with the first ensemble of high-resolution NWP model simulations in Saudi Arabia.
- 3) Investigating the sensitivity of wind resources estimates on the NWP setup (e.g., resolution and parameterizations applied) and choice of wind turbine specifications.

As part of our effort to provide an actionable and cost-efficient blueprint, we thoroughly discuss land-use restrictions and we identify the most suitable technological option for the different wind regimes experienced over the region.

2. Materials and methods

2.1. Wind speed model simulations

We quantify wind energy potential based on hourly high-resolution simulations of the Weather Research and Forecasting (WRF) model [28], applied over the Arabian Peninsula during 2013–2016. A set of WRF runs is generated to identify the optimal setup with respect to the spatial resolution, the planetary boundary layer (PBL) and surface layer schemes applied, which play a major role in dictating wind profiles in the boundary layer [29]. The simulation domain comprises 339×299 and 549×499 grid cells for the 9 km and 6 km resolution simulations, respectively (Table S1). The total surface area covered is roughly $8,200,000 \text{ km}^2$. WRF simulations include 40 vertical levels with varying vertical resolution, i.e., spaced closer together near the ground and becoming coarser as height increases. The layer of the atmosphere relevant to wind turbines (up to 200 m) is approximately discretized with a 20 m step. The WRF model is driven by initial and boundary conditions supplied by the operational high-resolution European Centre for Medium-Range Weather Forecast model (HRES-ECMWF) [30]. The boundary conditions are updated every 6 h. The non-hydrostatic dynamics equations are integrated without any nudging with a time step of 40 and 30 s for the simulations at 9 km and 6 km, respectively. For all the runs presented here, clouds and associated microphysical processes are represented with the Ferrier new Eta scheme [31], whereas the scale-aware Grell-Freitas convection scheme [32] represents the statistical effects of subgrid-scale convective clouds. Short and longwave radiation are parametrized with the Rapid Radiative Transfer Model for GCMs (RRMTG, [33]) and land surface processes are represented with the Noah land surface model [34]. A summary of the differences between the different runs in model setup (resolution and PBL schemes) is included in the Supplementary Information (Table S1).

2.2. Wind speed observations

We use the vertical profiles of wind speed measured at ten sites within the King Abdullah City for Atomic and Renewable Energy (K.A.CARE) monitoring network to evaluate model performance. For each site, P2546A Cup Anemometers were mounted onto a meteorological mast at different heights to measure wind speed at different heights (40, 60, 80 and 100 m). All K.A.CARE meteorological masts are 100 m high and have the same configuration and type of instruments. K.A.CARE wind data are aligned to international standards and guidelines to ensure data quality [35].

Hourly wind speed observations were collected from September 2013 until November 2016. However, the full time-span is covered by only a few stations, whereas measurements for all the sites are

simultaneously available only during 2016. Site-specific data coverage is reported in Table S2 and Fig. S1. The location of each measurement site is shown in Fig. 2.

2.3. Model performance evaluation

We evaluate WRF performance by pairing modeled and observed values in space using the nearest-neighbor approach, which is accomplished by identifying the closest grid cell to each observational site. The following performance indicators are used to assess the performance of the model:

$$MB = \frac{1}{N} \sum_{t=1}^N (\bar{W}_m(t) - \bar{W}_o(t)), \quad (1)$$

$$RMSE = \left(\frac{1}{N} \sum_{t=1}^N (\bar{W}_m(t) - \bar{W}_o(t))^2 \right)^{0.5}, \quad (2)$$

$$IOA = 1 - \frac{\sum_{t=1}^N (\bar{W}_m(t) - \bar{W}_o(t))^2}{\sum_{t=1}^N (|\bar{W}_m(t) - \bar{W}_0| + |\bar{W}_o(t) - \bar{W}_0|)^2}, \quad (3)$$

where \bar{W}_m is the sites-averaged modeled wind speed, \bar{W}_o is the sites-averaged observed wind speed, \bar{W}_0 is the sites and time averaged wind speed, t is the time coordinate and N is the number of observations. All indicators are computed with hourly data. Mean Bias (MB) aims to quantify systematic underestimation or overestimation, Root Mean Square Error (RMSE) is the standard deviation of the residuals and Index Of Agreement (IOA) is a standardized measure of the degree of model prediction error [36] and varies between 0 and 1. General guidelines for assessing the reliability of wind speed predictions in terms of the above-defined indicators are reported in Emery et al. [37] and are used as a reference for our model performance evaluation (MB within $\pm 0.5 \text{ m s}^{-1}$, RMSE lower than 2.0 m s^{-1} and IOA greater than 0.6).

2.4. Land-use restrictions

To account for the unsuitability of certain areas for wind power harvesting, we exclude from our analysis all the grid cells that are located in close proximity to urban areas, in extreme rugged terrain, in a wildlife reserve or adjacent to national borders.

In particular, we classify urban areas using the following procedure. First, we identify grid cells classified as “urban and built-up land” according to the USGS 24-categories land use data [38]. To properly consider the fast urbanization in Saudi Arabia over the past couple of decades, we also integrate information from the Landsat 2017 population dataset [39]. All the grid cells characterized by a population density higher than a fixed threshold are considered additional urban areas. We define this threshold as the minimum population density in the grid cells classified as “urban and built-up land” areas by USGS over Saudi Arabia ($934.9 \text{ inhabitants km}^{-2}$). Besides the 10 urban grid cells from the USGS classification, 123 additional grid cells are identified as urban areas based on the population density approach (Fig. S2a).

To account for the unsuitability of rugged areas, we compute the terrain ruggedness index (TRI) as defined in Riley et al. [40]. This index provides a quantitative measure of terrain ruggedness and is computed by summing the absolute values of changes in elevation between a grid cell and its eight neighboring grid cells. All the grid cells with higher TRI than a specific threshold are considered too rugged to be suitable for wind power. The threshold is set to the TRI value relative to a mountainous grid cell that contains the 117 MW Tafila Wind Farm in Jordan [41], as there are no wind farms currently built in Saudi Arabia. Based on this threshold (TRI = 891.2 m), we exclude 1800 grid cells from the computation for extreme ruggedness (Fig. S2c). As a comparison, we calculate that one of the most notorious alpine wind farm located in Steinriegel (Austria) has a TRI value equal to 708.9 m, which

is lower than our selected threshold. Excluding grid cells in rugged terrain is also a way to account for the additional installation costs that building turbines in such areas would entail. The reported values are specific for our resolution settings (i.e., to the 6 km resolution topography used in the WRF simulations) and are not intended to be generalizable in every context. In particular, for specific countries where mountainous areas are dominant, a careful selection of the TRI threshold should be performed before the analysis (based on other existing wind farms, as in this work, or on more refined criteria).

Furthermore, we identify and exclude wildlife reserves through the World Database on Protected Areas [42] as well as all the areas within a 50 km distance of national borders to avoid potential geopolitical concerns. A summary of all excluded areas can be found in the Supplementary Information (Fig. S2).

2.5. LCOE computation

LCOE is a measure of the total cost of building and operating a certain energy asset, divided by its total energy output over its entire lifetime, and is thus a crucial metric for assessing the cost-effectiveness of energy projects [43]. In this work, we calculate the LCOE for each grid cell and each possible combination of turbine model/hub height, following a recently published methodology specific for wind power potential assessments [44].

The total energy output (E_k) in grid cell k depends on the assumption of the turbine model and hub height, and it can be computed as the product of the installation potential (ϕ_k), the annual capacity factor of that grid cell (CF_k) and the hours of operation of the wind turbines (8760):

$$E_k = \phi_k CF_k \times 8760. \quad (4)$$

The installation potential (MW) depends on the power density (MW km^{-2}), i.e., how much power can be installed per unit surface. Following previous studies [45], the power density (ρ) is assumed to be:

$$\rho = \frac{P}{7D \times 5D}, \quad (5)$$

where P is the maximum rated power output and D is the rotor diameter. Given a certain grid cell size (A_k), the installation potential can be computed as:

$$\phi_k = \rho A_k. \quad (6)$$

The capacity factor at a grid cell k , CF_k , is computed as the annual average of the hourly wind power attainable for a given turbine model divided by the maximum rated power of the turbine. Turbine-specific power curves, as provided by the manufacturers, are used to convert hourly wind speed data given by the WRF model into hourly wind power, even though multiple other environmental factors may influence the actual power output [46]. However, a detailed assessment of the degree of uncertainty related to power curves, as well as the influence of extended wind farms [47], exceeds the scope of this work. Manufacturer power curves for each turbine are retrieved from The Wind Power Database [48]. Wind speed at hub height is computed by linearly interpolating the wind speed between the two closest WRF vertical levels.

In our assessment, we consider several wind turbines from different manufacturers, in order to (i) investigate the sensitivity of capacity factors to the chosen wind turbine and (ii) identify the most suitable wind turbines for the different wind regimes. We choose turbine models from leading manufacturers designed for different wind classes and whose power curves are available [48]. Technical details about the wind turbines considered in this work are reported in Table 1. The corresponding power curves are presented in Fig. S3.

Different sources are used to quantify the total lifetime costs of the potential wind energy projects. The total cost is estimated as the sum of the installation costs (I_k) and the operation and maintenance costs.

Table 1

Technical features of the turbines considered in our study.

Turbine model	Maximum rated power (kW)	Rotor diameter (m)	Rotor swept area (m ²)	Specific rating (W m ⁻²)	Feasible hub heights (m)
Vestas V110-2000	2000	110	9503	210	75, 80, 95, 110, 120, 125
Vestas V126-3450	3450	126	12,469	277	87, 117, 137, 147, 149, 166
GE 2.75–100	2750	100	7854	350	75, 85, 98.3, 123.5
GE 2.75–120	2780	120	11,310	243	90
GE 3.4–137	3500	137	14,741	230	85, 110, 131.4, 134, 164.5
Nordex N100-2500	2500	100	7823	318	75, 80, 100
Nordex N131-3300	3300	131	13,478	245	84, 106, 112, 114, 120, 134

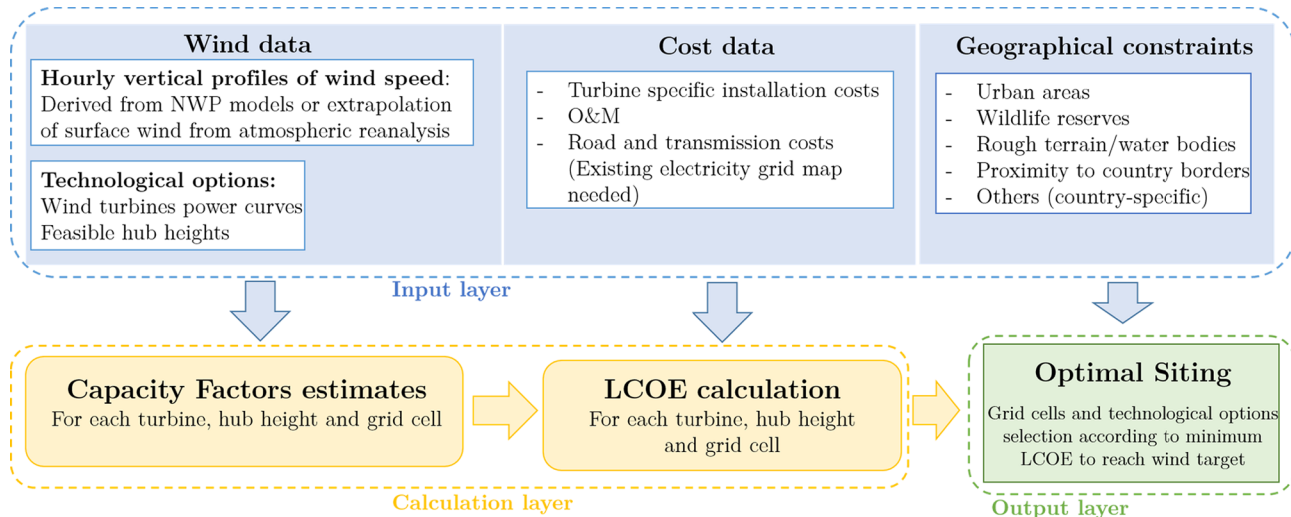


Fig. 1. General workflow for the methodology outlined from Section 2.1 to Section 2.6.

Installation costs include the turbine costs, which depend on the hub height (h) and the turbine specific rating (s), and all the costs related to new transmission lines and road construction to connect the turbine to the existing power grid (G_k). We adopt a linear relationship for turbine price (T_k , EUR kW⁻¹) based on European and US data, following Rinne et al. [44]:

$$T_k = \beta_1 \log(h) + \beta_2 s + C, \quad (7)$$

where $\beta_1 = 620$, $\beta_2 = -1.68$, $C = 1005$. We use the most recent five-year average USD EUR⁻¹ exchange rate of 1.15 for currency conversion. To compute G_k , we calculate the minimum distance to the existing electricity grid [49] for each grid cell and multiply the distance by the average costs of building transmission lines and roads per unit distance. The total installation cost is therefore:

$$I_k = \phi_k T_k + G_k = \phi_k (\beta_1 \log(h) + \beta_2 s + C) + G_k. \quad (8)$$

The average cost of building roads per unit distance is assumed to be 100 kUSD km⁻¹, following Saudi Arabia-specific literature [50], whereas transmission lines cost per unit distance is estimated to be 437 kUSD km⁻¹, based on a double circuit alternate current transmission [51]. As an example, applying Equation (8) to the planned wind farm in Dumyat al Jandal (99 units of Vestas V150-4.2 MW featuring 250 m-high towers) would result in an estimated installation cost of ~\$800 million, which is similar in magnitude to the planned cost (i.e., \$500 million [52]). The discrepancy between the installation costs might be due to the contingent agreement between the country and the contractors, as well as because T_k is based on US and European data. We finally compute LCOE as follows, for each grid cell k :

$$LCOE = \frac{I_k + \sum_{t=1}^T \frac{E_k O}{(1+r)^t}}{\sum_{t=1}^T \frac{E_k}{(1+r)^t}}, \quad (9)$$

where I_k and E_k are the installation costs and the annual energy

production computed above, respectively, O represents the operation and maintenance costs per year per unit of energy, r is a suitable discount rate and T is the expected lifetime of the turbines. Following Rinne et al. [44], we fixed $r = 5\%$ and $T = 20$ years. As there are no wind farms currently operating in Saudi Arabia, we use operation and maintenance costs from the United States (53 USD kW⁻¹ year⁻¹ or, equivalently, 12.1 USD MWh⁻¹, assuming a 0.5 capacity factor).

2.6. Optimal buildout calculation

To calculate the optimal wind farms buildout, we select grid cells with the minimum LCOE until the total installed capacity required by the wind target (16GW) is reached. We exclude from the analysis all the grid cells that are unsuitable for wind power generation due to (i) proximity to an urban area, (ii) presence of a wildlife reserve, (iii) extreme rugged terrain, and (iv) proximity to national borders, as detailed in Section 2.4 (Fig. S2). In our case study, we subdivide the total wind power capacity into the four main administrative regions of Saudi Arabia, proportionally to their electricity demand [49]. To account for the uncertainty of the costs (e.g., because they could vary considerably by country [53]), we perform a sensitivity analysis by simultaneously perturbing r , O and G_k in the range -75% , $+75\%$ with a 5% step size (i.e., in total $31 \times 31 \times 31$ different cost configurations were implemented). For each combination of the perturbed costs, the optimal configuration of wind farms is recalculated as well as the average LCOE of the selected grid cells. Finally, Fig. 1 summarizes the overall workflow of the methodology presented throughout Section 2.1 to 2.6.

3. Results

3.1. Numerical model simulations

Previous studies of wind energy potential over Saudi Arabia have

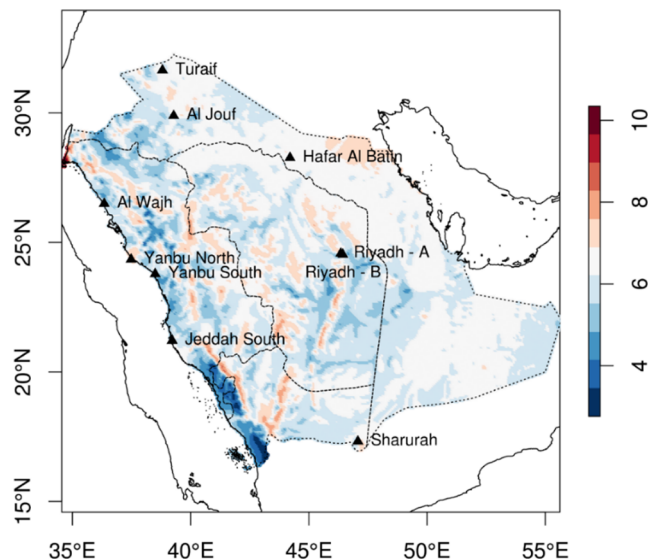


Fig. 2. Four-year average of wind speeds (m s^{-1}) at 80 m for the entire WRF domain (04–6 km-MYJ run). The black triangles indicate the locations of the K.A.CARE monitoring sites.

mostly relied either on measurements at individual selected locations (e.g., five coastal locations [22] and the Rafha area [54]) or on coarse global/regional model simulations [25] and reanalysis data [23], given the sparsity of observational data sources. Here, we develop a novel set of high-resolution model simulations that we use to investigate wind dynamics, as detailed in the Methods section. In the following discussion, we present results for the simulation that most accurately reproduces the observed wind dynamics at the ten measurement sites (04–6 km-MYJ run at 6 km resolution; Table S1), and in the Supplementary Information we report the sensitivity of the results against the WRF setup.

Fig. 2 displays the spatial distribution of wind speed at a typical hub height (80 m). The highest mean wind speeds are found along the western mountain ranges, which is in agreement with previous studies based on coarser resolution data [23]. Nonetheless, our high-resolution simulations identify new promising regions with high wind speeds in northwest Saudi Arabia, in close proximity to the borders with Jordan and Egypt, and near the Persian Gulf on the east coast. Resolving local scale physical phenomena (e.g., sea and land breezes) is thus critical to accurately characterize the spatial distribution of wind speed.

Minor changes across the four years of simulation are observed. Annual average wind speeds at 80 m across Saudi Arabia ranges from 6.3 m s^{-1} and 6.1 m s^{-1} in 2013 and 2016, respectively, and the spatial distribution remains almost unchanged throughout the domain (Fig. S4). Although our analysis is limited to four years, other studies based on output from the Middle East North Africa Coordinated Regional Climate Downscaling Experiment (MENA CORDEX) confirmed that wind speed interannual variability is low in the Arabian Peninsula [24].

We evaluate the performance of WRF in reproducing actual wind speeds by comparing the model results with observed wind speed data collected at different heights (40, 60, 80 and 100 m) at ten measurement sites (see Figs. S4–S7 for a comprehensive model performance evaluation). Fig. 3 shows the average daily 80 m wind speed during 2016, according to both the model and the observations. We select 2016 as the reference year for our evaluation because the entire set of data from all the measurement sites is available (Fig. S1). According to the performance metrics considered in this work – Mean Bias (MB), Root Mean Square Error (RMSE) and Index of Agreement (IOA), as detailed in the Methods section – the model accurately reproduces daily wind speeds and variability for all ten measurement sites, at every different altitude. Indeed, the model values are largely within the

bounds deemed acceptable for traditional wind speed performance evaluations [37], i.e., MB is in the range $\pm 0.5 \text{ m s}^{-1}$, RMSE is well below 2.0 m s^{-1} and IOA is well above 0.6. Furthermore, simulated diurnal profiles agree well with the observations for both inland and coastal locations, which is an indication that even at finer temporal resolution (i.e., hourly), WRF is able to capture the key wind speed characteristics (Figs. S5–S6).

3.2. Capacity factors

We compute the annual capacity factors for each combination of wind turbine and feasible hub heights. Fig. 4 shows the spatial distribution of four-year capacity factors for both low-rated and high-rated power Nordex turbines [48] (N100-2500 and N131-3300), at their respective lowest and highest hub heights, aiming to represent the whole spectrum of variability of the capacity factors. Previous attempts to estimate the wind power potential [23] have relied on extrapolations of 10 m wind speeds to the hub height, using the traditional logarithmic profile law [55]. No logarithmic extrapolation is needed in our work because the wind vertical profile is directly computed within the WRF model at a fine resolution (approximately 20 m) in the lowest portion of the planetary boundary layer. We obtain considerably different results when the capacity factors are computed using WRF output compared to the extrapolation method (Fig. S9), underlining that the commonly used power law approach is not an acceptable assumption in our case.

As expected, the spatial distribution of capacity factors across Saudi Arabia resembles the wind speed patterns at 80 m shown in Fig. 2. However, we identify considerable discrepancies between different combinations of turbine models and hub heights, highlighting the importance of employing a range of turbines suitable for different conditions, rather than using a single model only. As illustrated in Fig. 4, the capacity factor increases significantly from a 2.5 MW to a 3.3 MW turbine (average capacity factor from 0.288 to 0.375) because of an increase in turbine efficiency (i.e., the power curve shifts to the left for larger turbines). Due to larger wind speed available at higher altitudes, increasing the hub height also enhances capacity factors, although the rated power of the turbine seems to influence the capacity factors to a greater extent. Questions remain on whether the extra cost of building larger or taller wind turbines would be offset by the increase in energy produced. To this end, we include in our analysis a thorough cost assessment and we combine the two sets of information (i.e., potential energy and costs) through the LCOE indicator.

3.3. Optimal wind farms buildout

The optimal buildout can be calculated under two different scenarios. Firstly, we can assume one fixed combination of model turbine/height to calculate the LCOE and select the grid cells with minimum LCOE required to cover the wind target. Alternatively, we can identify the most suitable turbine for each grid cell across all possible combinations of turbine models and hub heights (i.e., the one characterized by the lowest LCOE, Fig. 5a), and then select the optimal grid cells to achieve the desired wind power capacity. The first calculation is clearly suboptimal, as it does not allow the selection of different turbine models and hub heights in different part of the country, which might experience different wind regimes. However, we expect a practical scenario to fall in between these two cases, as the installation of the new turbines would be highly dependent on the contingent agreement between the country and the contractors. As we find a limited variability in the optimal buildout across our four modelling simulations (Fig. S10), here we present only results for the most accurate simulation (04–6 km-MYJ run).

The comparison between these two approaches is shown in Fig. 6, in terms of the average LCOE for the selected grid cells and Saudi Arabia's annual electricity demand coverage, which was equal to 288.7 TWh in 2017 [49]. Each selected grid cell (36 km^2) should be regarded as a

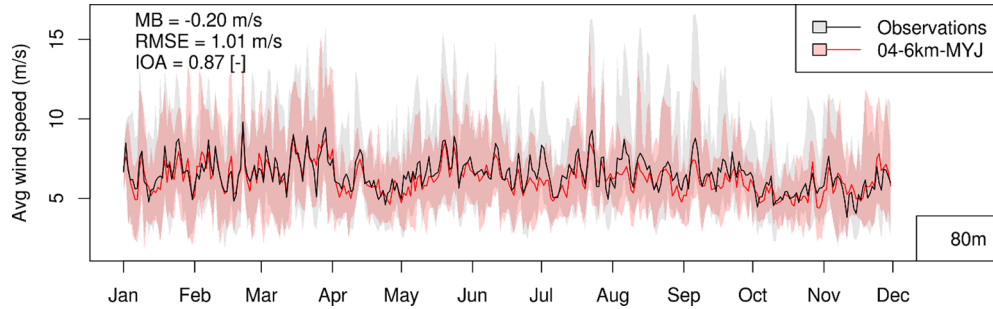


Fig. 3. Comparison between observed and modeled wind speeds for 2016 (04–6 km-MYJ run) at 80 m. Solid lines represent the site average and the shadings indicate the full variability (min-max) across the ten measurement sites.

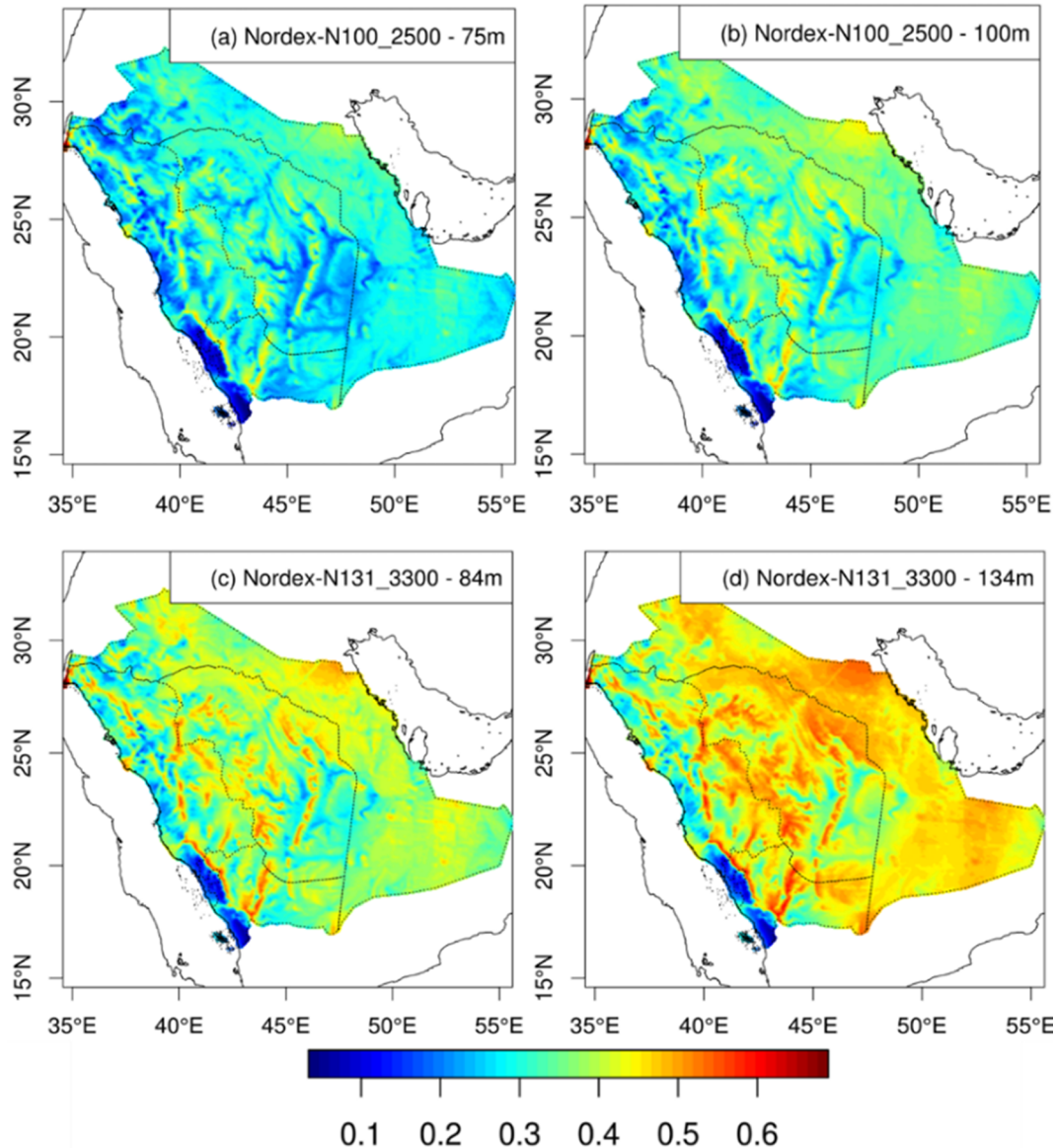


Fig. 4. Spatial distribution of capacity factors for different turbine models and hub heights, computed from data during the entire simulation period. Capacity factors refer to (a) Nordex N100-2500 at 75 m, (b) Nordex N100-2500 at 100 m, (c) Nordex N131-3300 at 84 m and (d) Nordex N131-3300 at 134 m.

single wind farm project, as the installed capacity per grid cell ranges between 198 and 283 MW, depending on the turbine model. The average LCOE for the optimal configuration of wind farms is ~ 39 USD MWh^{-1} , which is remarkably lower than the global average of 56.0 USD MWh^{-1} for 2018 wind energy projects [56]. As a comparison, the

most competitive bids submitted for Dumat Al Jandal wind project range from 21.3 to 33.9 USD MWh^{-1} , values in line with the average LCOE for the optimal configuration. Interestingly, our independent assessment provides results in accordance with the government's investment on the first wind project siting, as we also identify Dumat Al

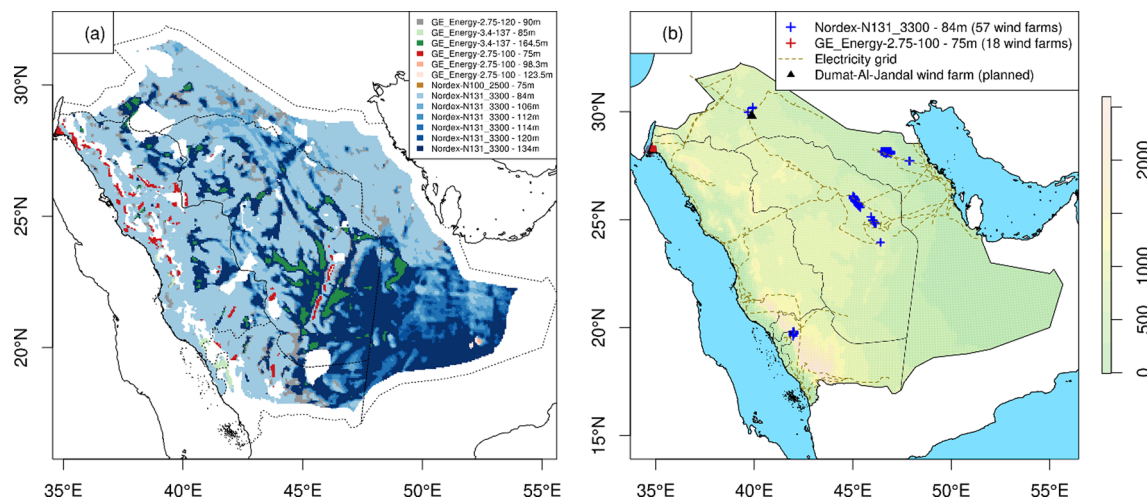


Fig. 5. (a) Optimal turbine model and hub height for each grid cell (04–6 km-MYJ run) and (b) optimal wind farms configuration obtained by employing different turbine models across the domain. The color scale indicate the altitude in meters above sea level. White areas in panel (a) are excluded from the calculations, either because they are outside Saudi Arabia's borders or because of unsuitability constraints (urban areas, wildlife reserves, rugged terrain or proximity to country borders).

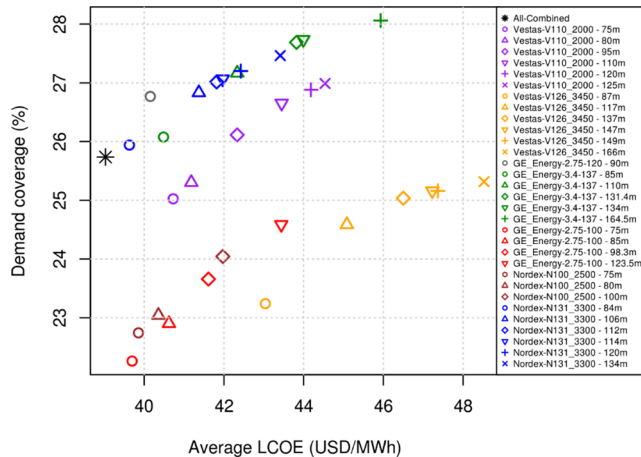


Fig. 6. Average LCOE (USD MWh^{-1}) and annual demand coverage (%) for each specific combination of turbine model and hub height. The black star (*all-combined*) refers to the optimal build-out obtained by allowing different turbines and hub heights for each simulated grid cell.

Jandal as one of the most cost-effective areas where wind projects should be tendered (Fig. 5b).

Our calculations show that approximately 26% of the 2017 Saudi Arabia's electricity demand could be met by optimally installing 16GW of wind power, assuming no wind energy curtailment. As expected, the second approach (*all-combined* in Fig. 6) attains the lowest average LCOE. Nevertheless, the benefits of using different turbines in each grid are rather limited, as only a few combinations of turbines and hub heights are consistently the most suitable for Saudi Arabia's wind regimes (as also highlighted by Fig. 5). The high-rated power Nordex turbine (*Nordex-N131-3300*) outperforms all other turbine models for most of Saudi Arabia's territory. Although larger turbines imply additional installation costs, we find that the benefits of having larger swept areas in terms of efficiency outweigh the additional costs. For the same reason, increasing the hub heights of wind turbines is optimal for locations characterized by very low wind speeds, where there is a considerable advantage in increasing the turbine height. The technological options selected by the optimization procedure indicate the main characteristics (e.g., specific rating, diameter, hub height, etc.) that a turbine should have for every wind regime experienced by each grid cell. Different turbines with similar characteristics are likely to have

similar performances in terms of LCOE, as illustrated by the sensitivity analysis presented in Figs. S11–S12. If the second (third) best combinations of turbine/hub height were chosen instead of the optimal one, the average LCOE for the entire Saudi Arabia would increase by around 0.46% (1.01%), respectively (Fig. S11). However, if the least suitable combinations were systematically chosen, the average LCOE over the entire domain would increase by 22.3%, which would clearly entail a suboptimal choice. Some regions appear to be more sensitive to the optimal choice with the increase in LCOE ranging from 21.7% to 142.9% when the least suitable turbine configurations are selected (Fig. S12). Overall, our results give indications on the main characteristics of the optimal turbines, but the final selection of the specific contractor may also depend on other factors (e.g., negotiations between parties), as the sensitivity of LCOE to similar turbines is rather small.

Fig. 6 also illustrates how the LCOE and the total annual energy produced are conflicting objectives, given a predefined amount of wind power capacity. Increasing the hub heights leads to higher annual demand coverages, but it negatively affects the average LCOE of the wind farms. We believe that the optimal configuration is the one that ensures minimum LCOE, as higher demand coverage could be most effectively reached in terms of cost by simply installing more capacity. Going beyond the 16GW target would not considerably affect the cost-effectiveness of the buildout, as illustrated in Fig. S13. As clear from the cumulative distribution function of optimal LCOE values, competitive LCOE values are achieved by approximately 6% of the total grid cells (Fig. S13), which correspond to installed capacities of around 400 GW (well above the 16GW target). The optimal characteristics of the selected 75 grid cells that are needed to achieve the 16GW target, for the *all-combined* approach, are reported in Table 2. Only two combinations of wind turbine and hub height are selected for the optimal 16GW configuration. The northwestern part of Saudi Arabia near the Gulf of Aqaba appears to be suitable for relatively small turbines at low hub height (*GE_Energy-2.75-100*) because of persistent high wind speeds even at low altitudes. Incidentally, the Gulf of Aqaba is also currently of high national interest because of the developing NEOM project, which is an envisioned new sustainable city that is intended to be pollution free and served entirely by renewable energy [57]. Larger turbines (*Nordex-N131-3300*) at low hub heights are instead more suitable in all the remaining optimal areas, which are mostly located along the power grid.

We assess the robustness of our results to the different cost configurations by repeating the analysis with simultaneously perturbed interest rate, O&M and road & transmission lines building costs from

Table 2

Summary of the optimal configuration of wind farms across all Saudi Arabia.

Turbine model	Number of wind farms (-)	Number of turbines per wind farm (-)	Total installed capacity (GW)	Total covered surface (km^2)	Annual energy production (TWh)
Nordex-N131-3300	57	60	11.3	2052	58.7
GE-Energy-2.75–100	18	103	5.10	648	16.1
Total	75	-	16.4	2700	74.8

–75% to +75% of their initial value, with a 5% step size (see the Methods for assumptions on the cost estimates). This sensitivity analysis shows that the average LCOE of the resulting buildouts ranges between 22.1 and 57.3 USD MWh^{-1} . Thus, competitive energy costs are reached even in the worst-case scenario (i.e., +75% of interest rate, O&M and road & transmission costs). The average LCOE is more sensitive to O&M costs and interest rate than to the road and transmission costs (Fig. S14), as the majority of the selected grid cells are located very close to the existing power grid. Furthermore, the optimal configuration of selected grid cells appears to be very robust for all the different possible cost alternatives (Fig. S15), which strongly indicates that the optimal areas identified in this work are not affected considerably by our cost assumptions.

4. Discussion

The presented WRF ensemble improves the characterization of wind speed patterns in Saudi Arabia compared to prior studies, and makes policy recommendations more actionable. The fine horizontal grid spacing (6 km) allows resolving local scale phenomena in the mean flow, thus identifying new promising locations for wind energy harvesting (e.g., the Gulf of Aqaba region has the lowest LCOE). These areas were not clearly highlighted by studies based on MERRA-2 reanalysis [23], MENA-CORDEX [24] and LENS [25] simulations due to their considerably coarser resolution. Furthermore, our high-resolution simulations provide a detailed characterization of the wind speed vertical profile within the planetary boundary layer (i.e., 9 model levels are present in the first 200 m above the ground), which facilitates the comparison and the selection of the optimal turbine model and hub height.

Sources of uncertainty that require further investigation (beyond the scope of this work) include turbine degradation [58], the role of dust [59] and the wake effect [60] on real wind turbine operation and energy production. Sand storms are particularly frequent in Saudi Arabia [61] and more experimental [62] and modelling studies [63] are needed to quantify the possible impact of sand storms on turbine operation. Wind power production may be also affected by wind farm design and the location of individual turbines. The wake effect has been the focus of several recent studies that have indicated minor downwind impacts on weather and climate features [64] and thus on capacity factors [65]. The proximity of several wind farms to each other, as proposed by the optimal buildout here, may generate a sequence of wakes [60] whose impact should be investigated and quantified in subsequent modelling studies. As a result, capacity factors calculated in this work are likely to be greater than the real ones, which entails that the overall LCOE values are presumably slightly underestimated (i.e., they represent a theoretical value assuming no energy losses due to wake effect and no decay in turbine performances during their lifetimes). Nonetheless, the optimal configuration of wind farms would not be affected by such assumptions, since the relative differences in LCOE between different locations do not depend on spatially uniform energy losses.

Even more wind power generation could be achieved by expanding the installed power capacity in nearby areas. Indeed, approximately 40% of Saudi Arabia's 2017 electricity demand could be met by installing 25GW of wind power (see Fig. S16 for optimal wind farm

configuration), without significantly affecting the cost-effectiveness of the buildup (Fig. S13). As both population and electricity demand are on the rise in Saudi Arabia [16], higher installed capacity would be required to meet the excess demand and keep the annual demand coverage by wind power steady. We foresee that investments beyond the Vision 2030 will be physically achievable as the projected wind spatial patterns in future climates are coherent with the current one [24].

The present study only focuses on harvesting renewable energy from wind, but a more thorough plan for sustainable and clean energy development should consider deployment of offshore wind turbines or incorporate other energy resources, such as solar power. Abundant solar resources are indeed available in Saudi Arabia, given its location in the sun belt [66]. As shown in Fig. S17, the highest wind power is attainable during nighttime for our proposed buildup, whereas solar power peaks during daytime. These diurnal variations could complement each other if both wind and solar power systems are effectively integrated. Future studies will be thus devoted to investigating ways to integrate these two key resources, with the final aim of understanding if only wind and solar energy could meet the hourly demand at least for specific regions of Saudi Arabia.

The presented framework relies on high-resolution and detailed NWP simulations for turbine/hub heights selection and proper identification of the most suitable areas. Although we acknowledge that such simulations are not yet available worldwide, recent efforts in global model simulations have achieved unprecedented horizontal resolution [67], and computational resources have become increasingly more available. Moreover, ongoing research is devoted to developing improved techniques for the vertical extrapolation of surface wind speeds [68] which may lead in the near future to an improved characterization of the wind vertical profiles without requiring expensive regional high-resolution NWP simulations.

5. Conclusions

In this work we set forth a practical and general modelling framework to bridge the gap between wind energy policy targets and their implementation. We exemplify such methodology for Saudi Arabia's ambitious wind energy investment plans. By using novel high-resolution numerical weather prediction model simulations, we identify the optimal locations for wind farms and the most suitable combination of turbine models and hub heights across the country. Coastal areas along the Gulf of Aqaba, in the northwestern part of the country, offer the most cost-effective wind resource potential. The optimal distribution of wind farms could generate up to 26% of Saudi Arabia's electricity demand (based on 2017 levels of energy consumption). Our results demonstrate for the first time that Saudi Arabia can achieve its renewable wind energy targets at a very competitive levelized cost of energy. We argue that Saudi Arabia is well positioned to be a role model for wind energy development within the Middle East and other emerging countries, shall the wind energy blueprint outlined here be implemented. The modelling framework presented here can prove useful for other countries aiming to strengthen their wind energy infrastructure.

CRediT authorship contribution statement

Paolo Giani: Conceptualization, Methodology, Investigation, Formal analysis, Software, Writing - original draft. **Felipe Tagle:** Conceptualization, Methodology, Writing - review & editing. **Marc G. Genton:** Writing - review & editing, Supervision, Project administration. **Stefano Castruccio:** Methodology, Writing - original draft, Supervision. **Paola Crippa:** Conceptualization, Resources, Investigation, Supervision, Writing - original draft.

Declaration of Competing Interest

The authors declare no competing interests.

Acknowledgements

This publication is based upon work supported by the King Abdullah University of Science and Technology (KAUST) Office of Sponsored Research (OSR) under Award No: OSR-CRG 7 2018-3742.2. This work utilized the LandScan (2017) High Resolution global Population Data Set copyrighted by UT-Battelle, LLC, operator of Oak Ridge National Laboratory under Contract No. DE-AC05-00OR22725 with the United States Department of Energy.

HRES-ECMWF operational analysis data were downloaded from the ECMWF data portal (<https://www.ecmwf.int/en/forecasts/datasets/set-i>) through the KAUST ECMWF licence. The authors thank the King Abdullah City for Atomic and Renewable Energy (K.A.CARE) for providing the wind speed observational data. PG acknowledges support from the Richard and Peggy Notebaert Premier Fellowship.

Appendix A. Supplementary material

Supplementary data to this article can be found online at <https://doi.org/10.1016/j.apenergy.2020.115085>.

References

- [1] IPCC. Climate change 2014–Impacts, adaptation and vulnerability. Part A: Global and Sectoral Aspect. 2014: Cambridge University Press.
- [2] Armstrong RC, Wolfram C, De Jong KP, Gross R, Lewis NS, Boardman B, et al. The frontiers of energy. *Nat Energy* 2016;1(1):1–8.
- [3] Kinley R. Climate change after Paris: from turning point to transformation. *Climate Policy* 2017;17(1):9–15.
- [4] REN21. Renewables 2018 - Global Status Report. Paris, REN21 Secretariat, 2018.
- [5] EIA. Annual Energy Outlook 2017 with projections to 2050, U.S.E.I. Administration, Editor. 2017, U.S. Energy Information Administration. p. 64.
- [6] Lidula N, Mithulanthan N, Ongsakul W, Widjaya C, Henson R. ASEAN towards clean and sustainable energy: Potentials, utilization and barriers. *Renewable Energy* 2007;32(9):1441–52.
- [7] Verbruggen A, Fischedick M, Moomaw W, Weir T, Nadai A, Nilsson LJ, et al. Renewable energy costs, potentials, barriers: Conceptual issues. *Energy policy* 2010;38(2):850–61.
- [8] Al-Badi A, Malik A, Gastli A. Assessment of renewable energy resources potential in Oman and identification of barrier to their significant utilization. *Renew Sustain Energy Rev* 2009;13(9):2734–9.
- [9] Sahir MH, Qureshi AH. Assessment of new and renewable energy resources potential and identification of barriers to their significant utilization in Pakistan. *Renew Sustain Energy Rev* 2008;12(1):290–8.
- [10] Jacobson MZ, Delucchi MA. Providing all global energy with wind, water, and solar power, Part I: Technologies, energy resources, quantities and areas of infrastructure, and materials. *Energy Policy* 2011;39(3):1154–69.
- [11] Zhang H, Cao Y, Zhang Y, Terzija V. Quantitative synergy assessment of regional wind-solar energy resources based on MERRA reanalysis data. *Appl Energy* 2018;216:172–82.
- [12] Evans JP, Kay M, Prasad A, Pitman A. The resilience of Australian wind energy to climate change. *Environ Res Lett* 2018;13(2):024014.
- [13] Liu F, Sun F, Liu W, Wang T, Wang H, Wang X, et al. On wind speed pattern and energy potential in China. *Appl Energy* 2019;236:867–76.
- [14] Fant C, Gunturu B, Schlosser A. Characterizing wind power resource reliability in southern Africa. *Appl Energy* 2016;161:565–73.
- [15] Griffiths S. A review and assessment of energy policy in the Middle East and North Africa region. *Energy Policy* 2017;102:249–69.
- [16] K.A.CARE. Building the renewable energy sector in Saudi Arabia. 2012.
- [17] Nurunnabi M. Transformation from an oil-based economy to a knowledge-based economy in Saudi Arabia: the Direction of Saudi Vision 2030. *J Knowledge Econ* 2017;8(2):536–64.
- [18] NREP. Saudi Arabia Renewable energy targets and long term visibility. National Renewable Energy Program; 2018.
- [19] GWEC. Global Wind Report 2018, Global wind energy council, Brussels, Belgium; 2019.
- [20] Masdar. The EDF Renewables-Masdar consortium awarded the Dumat Al Jandal (400 MW) wind project in Saudi Arabia Masdar, Accessed March 16th, <https://masdar.ae/en/masdarclean-energy/projects/dumat-al-jandal>, 2020.
- [21] Timmerberg S, Sanna A, Kaltchmitt M, Finkbeiner M. Renewable electricity targets in selected MENA countries–Assessment of available resources, generation costs and GHG emissions. *Energy Rep* 2019;5:1470–87.
- [22] Rehman S, Ahmad A. Assessment of wind energy potential for coastal locations of the Kingdom of Saudi Arabia. *Energy* 2004;29(8):1105–15.
- [23] Yip CMA, Gunturu UB, Stenchikov GL. Wind resource characterization in the Arabian Peninsula. *Appl Energy* 2016;164:826–36.
- [24] Chen W, Castruccio S, Genton MG, Crippa P. Current and future estimates of wind energy potential over Saudi Arabia. *J Geophys Res: Atmospheres* 2018;123(12):6443–59.
- [25] Tagle F, Castruccio S, Crippa P, Genton MG. A Non-Gaussian Spatio-temporal model for daily wind speeds based on a multi-Variate skew-t distribution. *J Time Ser Anal* 2019;40(3):312–26.
- [26] Kay JE, Deser C, Phillips A, Mai A, Hannay C, Strand G, et al. The Community Earth System Model (CESM) large ensemble project: A community resource for studying climate change in the presence of internal climate variability. *Bull Am Meteorol Soc* 2015;96(8):1333–49.
- [27] Tagle Felipe, Genton Marc, Yip Andrew, Mostamandi Suleiman, Stenchikov Georgiy, Castruccio Stefano. A high-resolution bilevel skew-t stochastic generator for assessing Saudi Arabia's wind energy resources. *Environmetrics* 2020.
- [28] Skamarock WC, Klemp JB, Dudhia J, Gill DO, Barker DM, Duda MG, et al. A description of the advanced research WRF version 3, NCAR Technical Note. National Center for Atmospheric Research: Boulder, CO, USA; 2008.
- [29] Gomez JJ, Raible C, Dierer S. Sensitivity of the WRF model to PBL parametrizations and nesting techniques: evaluation of wind storms over complex terrain. *Geoscientific Model Devel (GMD)* 2015;8(10):3349–63.
- [30] ECWRF. ECMWF IFS CY41r2 High-Resolution Operational Forecasts, edited, Research Data Archive at the National Center for Atmospheric Research, Computational and Information Systems Laboratory, Boulder, CO; 2016.
- [31] Ferrier BS, Lin V, Black F, Rogers E, DiMego G, Jin Y. Implementation of a new grid-scale cloud and precipitation scheme in the NCEP Eta model; 2002.
- [32] Grell GA, Freitas SR. A scale and aerosol aware stochastic convective parameterization for weather and air quality modeling. *Atmos Chem Phys* 2014;14(10):5233–50.
- [33] Iacono MJ, Delamere JS, Mlawer EJ, Shephard MW, Clough SA, Collins WD. Radiative forcing by long-lived greenhouse gases: Calculations with the AER radiative transfer models. *J Geophys Res: Atmosph* 2008;113(D13).
- [34] Tewari M, Chen F, Wang W, Dudhia J, LeMone M, Mitchell K, et al. Implementation and verification of the unified NOAH land surface model in the WRF model. In: 20th conference on weather analysis and forecasting/16th conference on numerical weather prediction. 2004. American Meteorological Society Seattle, WA; 2004.
- [35] MEASNET. Evaluation of Site-Specific Wind Conditions. Measuring Network of Wind Energy Institutes (MEASNET), Madrid, Spain; 2009.
- [36] Willmott CJ. On the validation of models. *Phys Geogr* 1981;2(2):184–94.
- [37] Emery C, Tai E, Yarwood G. Enhanced meteorological modeling and performance evaluation for two Texas ozone episodes. Prepared for the Texas natural resource conservation commission, by ENVIRON International Corporation; 2001.
- [38] Anderson JR. A land use and land cover classification system for use with remote sensor data. vol. 964. US Government Printing Office; 1976.
- [39] Rose A, McKee JJ, Urban M, Bright E. LandScan 2017. Oak Ridge, TN: Oak Ridge National Laboratory; 2018.
- [40] Riley SJ, DeGloria SD, Elliot R. Index that quantifies topographic heterogeneity. *Intermount. J. Sci.* 1999;5(1–4):23–7.
- [41] Al-Addous M, Al-Taani H, Dalalah Z, Alawneh F, Albatayneh A. Wind resource assessment for a proposed wind farm. In: Advanced studies in energy efficiency and built environment for developing countries. Springer, 2019. p. 179–189.
- [42] UNEP-WCMC I. Protected Planet: the World Database on Protected Areas (WDPA). UNEP-WCMC and IUCN, Cambridge, UK Available at: <http://www.protected-planet.net>, Accessed March 2019, 2019. 21.
- [43] Ueckerdt F, Hirth L, Luderer G, Edenhofer O. System LCOE: What are the costs of variable renewables? *Energy* 2013;63:61–75.
- [44] Rinne E, Holttinen H, Kiviluoma J, Rissanen S. Effects of turbine technology and land use on wind power resource potential. *Nat Energy* 2018;3(6):494.
- [45]IRENA. Wind power spatial planning techniques Global Atlas Training on Planning the Renewable Energy Transition Using Solar and Wind Maps Session 2a; 2015.
- [46] Lee G, Ding Y, Genton MG, Xie L. Power curve estimation with multivariate environmental factors for inland and offshore wind farms. *J Am Stat Assoc* 2015;110(509):56–67.
- [47] Staffell I, Pfenninger S. Using bias-corrected reanalysis to simulate current and future wind power output. *Energy* 2016;114:1224–39.
- [48] TheWindPower. Power Curves Database, Accessed April 2019 (The Wind Power, www.thewindpower.net); 2019.
- [49] SEC. Annual report 2017 - Saudi Electricity Company, URL = <https://www.se.com.sa/en-us/Pages/AnnualReports.aspx>; 2017.
- [50] IMF. IMF Country Report No. 14/188 - United Arab Emirates, International Monetary Fund; 2014.
- [51] IEA-ETSP. Technology Brief E12 - Electricity Transmission and Distribution,

- International Energy Agency - Energy Technology Systems Analysis Program; 2014.
- [52] IRENA. Renewable Energy Market Analysis (GCC 2019). Accessed March 16th, https://www.irena.org/-/media/Files/IRENA/Agency/Publication/2019/Jan/IRENA_Market_Analysis_GCC_2019.pdf, 2019.
- [53] Thornton G, Pipeline CE. Renewable energy discount rate survey results–2017. Grant Thornton and Clean Energy Pipeline Initiative, Grant Thornton UK LLP; 2018.
- [54] Rehman S, El-Amin I, Ahmad F, Shaahid S, Al-Shehri A, Bakhshwain J. Wind power resource assessment for Rafha, Saudi Arabia. *Renew Sustain Energy Rev* 2007;11(5):937–50.
- [55] Pryor S, Barthelmie R. Assessing climate change impacts on the near-term stability of the wind energy resource over the United States. *Proc Natl Acad Sci* 2011;108(20):8167–71.
- [56] IRENA. Renewable Power Generation Costs in 2018, International Renewable Energy Agency, Abu Dhabi; 2019.
- [57] Farag AA. The Story of NEOM City: opportunities and challenges. New Cities and Community Extensions in Egypt and the Middle East; 2019: p. 35–49.
- [58] Jia X, Jin C, Buzzo M, Wang W, Lee J. Wind turbine performance degradation assessment based on a novel similarity metric for machine performance curves. *Renewable Energy* 2016;99:1191–201.
- [59] Fiore G, Selig MS. Simulation of damage for wind turbine blades due to airborne particles. *Wind Eng* 2015;39(4):399–418.
- [60] Lundquist J, DuVivier K, Kaffine D, Tomaszewski J. Costs and consequences of wind turbine wake effects arising from uncoordinated wind energy development. *Nat Energy* 2019;4(1):26–34.
- [61] Notaro M, Alkolibi F, Fadda E, Bakhray F. Trajectory analysis of Saudi Arabian dust storms. *J Geophys Res: Atmosph* 2013;118(12):6028–43.
- [62] Khalfallah MG, Koliub AM. Effect of dust on the performance of wind turbines. *Desalination* 2007;209(1–3):209–20.
- [63] Schramm M, Rahimi H, Stoevesandt B, Tangager K. The influence of eroded blades on wind turbine performance using numerical simulations. *Energies* 2017;10(9):1420.
- [64] Pryor S, Barthelmie R, Shepherd T. 20% of US electricity from wind will have limited impacts on system efficiency and regional climate. *Sci Rep* 2020;10(1):1–14.
- [65] Pryor S, Barthelmie R, Hahmann A, Shepherd T, Volker P. Downstream effects from contemporary wind turbine deployments. *J Phys Conf Ser* 2018;1037(7):072010.
- [66] Saleh H. Evaluation of solar energy research and its applications in Saudi Arabia — 20 years of experience. 2001;5: 59–77.
- [67] Haarsma RJ, Roberts MJ, Vidale PL, Senior CA, Bellucci A, Bao Q, et al. High resolution model intercomparison project (HighResMIP v1. 0) for CMIP6. *Geosci Model Dev* 2016;9(11):4185–208.
- [68] Gualtieri G. A comprehensive review on wind resource extrapolation models applied in wind energy. *Renew Sustain Energy Rev* 2019;102:215–33.